# Magnetic and Electric Characterization of Materials for Electrical Machines

M.S.Muhit[1], Rashedul hoque[2]

**Abstract**— This paper aims to reflect over characterization of materials for electrical machines. Electromagnetic properties (b-h curves) and electrical resistivity were the main properties investigated in the project work. As the sample, rings made of steel used for structural pieces in large AC machine have been chosen. The ring samples (structural steel) are characterized to explore the B-H curves at frequencies in the range [0.1-250 Hz] and field intensity up to 900 A/m. For resistivity measurements, standard resistivity measurement techniques have been implemented based on proposed analytical equations.

**Index Terms**— Magnetic properties, hysteresisgraph,core loss , soft magnetic material, electrical steel, resistivity measurement.

————————————— ◆ —————————————

## 1  INTRODUCTION

ROTATING electrical machines are commonly built with different grades of iron, steel and other metallic alloys. The stator and rotor are commonly built with specific grades of laminated electrical steel. Proper dimensioning of the machine requires precise estimation of the B-H curves of the laminations and also the iron loss it undergoes during various states of operation. Lamination sheets are usually ordered with specific grades from the manufacturer. The grades describe material characteristics and losses at two operating points at least (f=50, 60 Hz and B=1, 1.5 T). These loss characteristics may not be sufficient for machines with variable speed drives or with different types of excitation supply. Hence, it requires characterization over wide frequency ranges (0.1-1000 Hz) and varying magnetic field levels (50-500 A/m) high enough to reach saturation flux density. Beside lamination sheets, structural metallic parts are used in the machine for several purposes. Some of these parts are also subjected to flux density variations if they happen to be placed in leakage flux paths. Hence they may undergo eddy current and hysteresis losses too. Due to lack of material characterization, these losses are usually not accounted in the simulation models. Hence, efficiency is not accurately calculated. To include the structural materials in loss calculation model, they require characterization.

This paper aims to describe the activities conducted to measure the magnetic characteristics and loss figures under sinusoidal excitation of a specific part of the electric machine, especially manufactured rings made of steel used for structural parts. Electrical characterization has been done to measure the resistivity values of the samples. The results [1] described in this paper are based upon experiments performed in the electromagnetic engineering lab and electrical machines lab of Royal Institute of technology – KTH, Stockholm, Sweden.

————————————————

1.  *M.S.Muhit has completed his Msc in electric Power Engineering from Royal Institute of technology, Stockholm, Sweden. E-mail:muhit@kth.se*

2.  *Rashedul Hoque has completed his Msc in wireless communication from Lund University, Lund, Sweden. E-mail: awi10rho@student.lu.se*

## 2  MAGNETIC CHARACTERIZATION

Characterization of soft magnetic materials aims at defining a given material's suitability on being selected for a particular application [2]. In simple terms, magnetic characterization can be explained as an experimental procedure in which the specimens made of the investigated material are subjected to wide range of polarization levels at different frequencies. Among other parameters, magnetic losses at different frequency and induction levels, relative permeability (µr) and coercivity (Hci) are of significant interest.

### 2.1 Hysteresisgraph Measurements

The response of magnetic materials can vary greatly with applied magnetic field. To obtain desired characteristics, controlled magnetic field must be applied. A commonly used instrumental setup facilitating the measurements is a hysteresisgraph or BH meter [3]. Test specimens defining closed magnetic loop are equipped with an excitation winding and a measurement winding. The response is measured at varying magnetic field strength and frequency. Result of the measurement is a hysteresis curve. Figure 1 displays a typical setup.
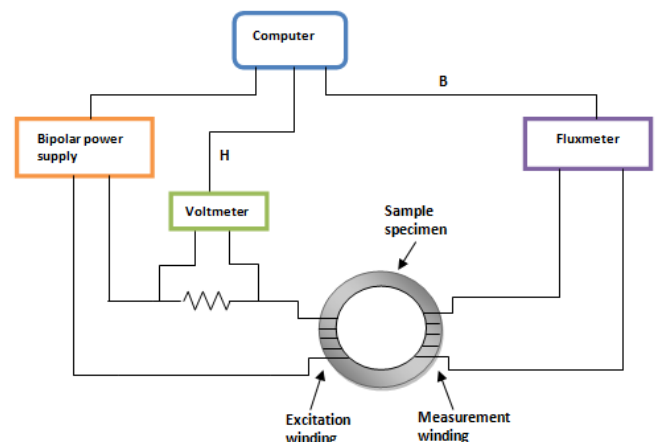


Fig. 1 Typical hysteresisgraph setup for characterization of soft magnetic materials

An AC sinusoidal current is injected into the excitation winding which induces a magnetic field H in the sample. The value of current is obtained from the measured voltage drop across the shunt resistor. The value of applied magnetic field H is directly proportional to the current according to line integral form of Ampere's law.

$$\hat{H} = \frac{N_1}{l_m}\hat{I}_1 \qquad (1)$$

Where,

$\hat{H}$    is peak magnetic field strength in A/m

$N_1$    is the total number of turns in the excitation winding

$l_m$    is the effective magnetic path length of the test specimen

$\hat{I}_1$    is the peak value of the magnetizing current

The applied magnetic field in the excitation coil gives rise to voltage across the measurement winding. The induced voltage is integrated over time to obtain the induced flux density (B) using a fluxmeter.

$$V_{rms} = \sqrt{2}\pi f N_2 A B_{max} \qquad (2)$$

Where

$V_{rms}$    is the rms value of the induced voltage in measurement winding in V.

$N_2$    is the total number of turns in the measurement winding.

A    is the cross sectional area of the test specimen in $m^2$ (value given as input to fluxmeter).

F    is the frequency in Hz.

$B_{max}$    is the peak flux density obtained by flux meter in T.

The computer interface allows conducting controlled magnetic measurements. B and H can be simultaneously measured using a data acquisition card. To obtain initial b-h characteristics curve, the sample needs to be demagnetized in a decreasing alternating field to begin with. The obtained curves are often used as input properties of magnetic materials in modeling of electro-mechanical devices, finite element simulations being one of the possibilities.

## 2.2 Hysteresis Curve

The resulting plot of a hysteresisgraph measurement is the B-H characteristics curve as shown in figure 2.
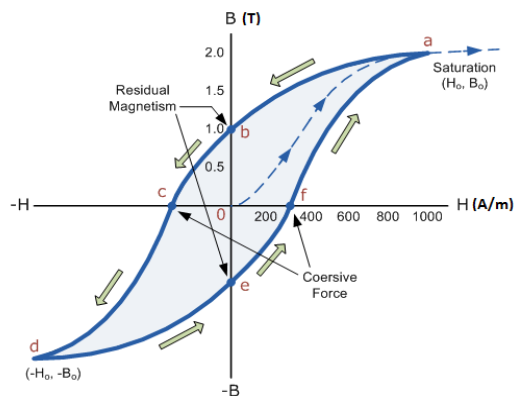


Fig. 2 Hysteresis loop

Important properties of the soft magnetic material are obtained in points be, cf , a and d shown in figure 2. The total area enclosed by hysteresis loop abcdef is a measure of hysteresis loss in one cycle per unit volume of the material as in equation 3.

$$Total\ loss(W/Kg) = \frac{obtained\ area * frequency}{density\ of\ material} \qquad (3)$$

## 2.3 Digital feedback control loop

According to international standard, power loss measurement in magnetic materials must be recorded only under sinusoidal flux density [4]. But magnetic materials are non linear due to inherent hysteresis characteristics of the material. Hence controlled feedback must be used to retain sinusoidal flux density [5]. For traditional measurements analog feedback is sufficient enough. Problem arises when measurements are taken over wide range of polarization levels at high frequencies. In these cases, the feedback loop needs high performance. According to [5], digital feedback is then to be preferred. Sinusoidal flux density is obtained by iterative modification of the magnetizing current. Such a solution is discussed in [5]. Computers equipped with LabVIEW® or dSPACE software incorporated with a high speed data acquisition system consisting of DAQ (data acquisition and generation card) are used during measurements. Figure 3 shows a general setup of magnetization of samples under controlled feedback loop.
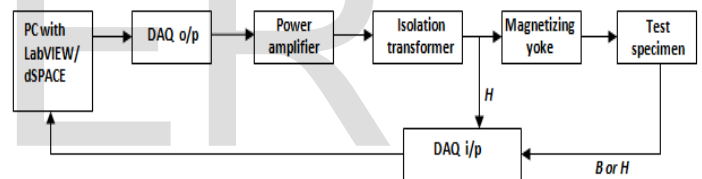


Fig. 3 Block diagram of magnetizing systems with closed loop feedback

Generated voltage from the data acquisition card is fed to an isolation transformer through a power amplifier. The transformer removes dc component present in the output current. The current fed into the magnetizing yoke is measured using the voltage drop across shunt resistor. The value of magnetic field is proportional to current, whose instantaneous value is fed into the inputs of DAQ. The induced flux density in the test specimen is obtained from the B sense coils surrounding the test specimen.

Using adaptive digital iterative feedback algorithm, the magnetizing current is continuously modified to retain sinusoidal output flux density. This type of algorithm serves as superior alternative to other type of digital feedback due to high stability and adaptive potential to various magnetizing systems.

## 2.4 Iron loss in electrical machines

In electrical machines, iron loss occurs in stator teeth, stator core and rotor core [6]. To reduce eddy currents, laminated steel of different grades can be used in the construction of stator and rotor cores. The choice of steel grade can greatly reduce iron losses hence increase efficiency. In most cases the

datasheet consist of loss figures at different induction level with sinusoidal variations of the flux density. A typical loss calculation model can be:

$$P_{loss} = P_{hyst} + P_{eddy} + P_{excess}$$

$$= k_h B^2 f + \frac{\pi^2 \sigma d (fB)^2}{6} + k_c (fB)^{\frac{3}{2}} \qquad (4)$$

Where
$k_h, k_c$    are the loss coefficients
   d     is the lamination thickness in mm
   σ     is the material conductivity in Sm-1
   f     is the frequency in Hz
   B     is the peak flux density in T

Hysteresis loss is also termed as static loss. It is independent of rate of change (e.g. frequency) of flux.

The eddy current and excess loss components are highly rate dependent. Hence the b-h curve broadens as shown in figure 4 [7]. $H_{stat}$ = Hysteresis loss, is represented as solid line. $H_{stat}$ + $H_{eddy}$ shown by dashed line. The dotted line represents the total iron loss.
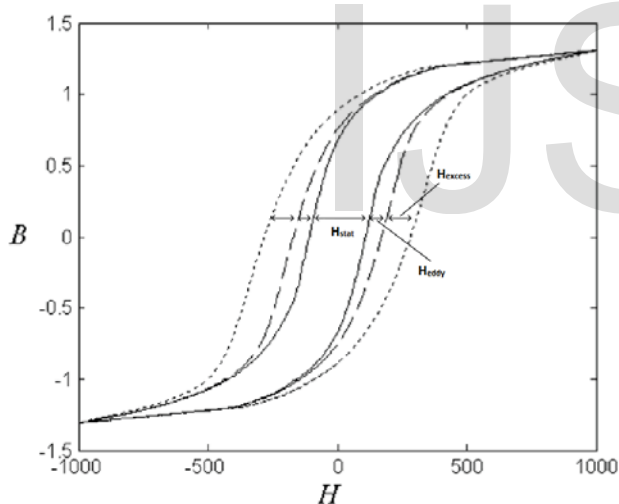


Fig. 4 Composition of dynamic magnetization curve at moderate frequencies for electrical steels [7]

## 3 MAGNETIC CHARACTERIZATION OF RING SAMPLE

The stator lamination sheets are usually stacked together and bolted at ends with 'metallic structures'. These conducting and magnetic parts are also subjected to sinusoidal flux density inducing eddy currents. Analyzing core loss in those parts also turned out to be a matter of interest. As these materials do not have any grade or characteristics data, they were selected for magnetic characterization [1]. Construction steel was used to machine circular ring samples. This was the only significant information available before characterization tests. Regarding magnetic properties of the material, no information was available since it is not intended to be used in magnetic circuit.

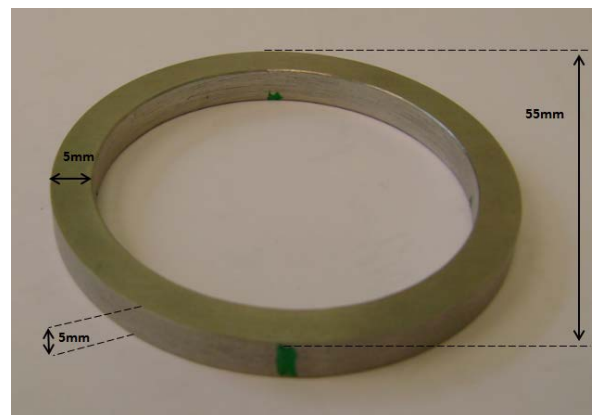Figure 5 shows a photograph of the sample.



Fig. 5 Sample of construction steel

To test the specimen with closed magnetic path, the hysteresisgraph principle discussed in section 2.1 has been followed.

### 3.1 Test fixture and sample preparation

Two samples were prepared for analyzing the magnetic characteristics. For the excitation winding wires of diameter 0.95 mm (±1%) was used. In the measurement winding, a comparatively thinner wire of diameter 0.145 mm (±1%) has been used. The wire diameters were measured using a micrometer screw gauge of accuracy 0.01 mm. The choice of thicker wires in the excitation winding side allows for higher current injection without heating the sample specimen. The samples were wounded by hand. The number of turns in the excitation winding was chosen on basis of Ampere's law. For measurement winding, on basis of Faraday's law of induced emf the number of turns have been chosen. Insulation tape (of negligible thickness and no magnetic properties) is wound around the sample to prevent short circuit between the sample and windings to be wound on top. Then, using the thinner wires, measurement winding was placed. One more layer of insulation tape is put over the measurement winding. Finally, the excitation winding is wounded over the insulation layer. Winding the excitation winding outside the measurement winding reduces the influence of stray field from outside. Table 1 shows winding turns for the prepared samples.

TABLE 1
WINDING INFORMATION FOR SAMPLES

|  | Sample 1 | Sample 2 |
|---|---|---|
| **Excitation winding turns** | 116 | 136 |
| **Measurement winding turns** | 492 | 533 |
| $R_{measurement}$ **(Ω)** | 0.236 | 0.273 |
| $R_{excitation}$ **(Ω)** | 6.38 | 6.915 |

The ends of the windings are soldered with connecting pins to allow current injection and voltage measurement. To enhance rigidity of the connections, a framework has been used.

## 3.2 Test bench setup arrangement

The test bench arrangement is exactly the same as in section 4.1.4 [1]. The only difference is the replacement of the test fixture (the Epstein frame) with the wounded ring samples. Figure 6 displays the setup arrangement.
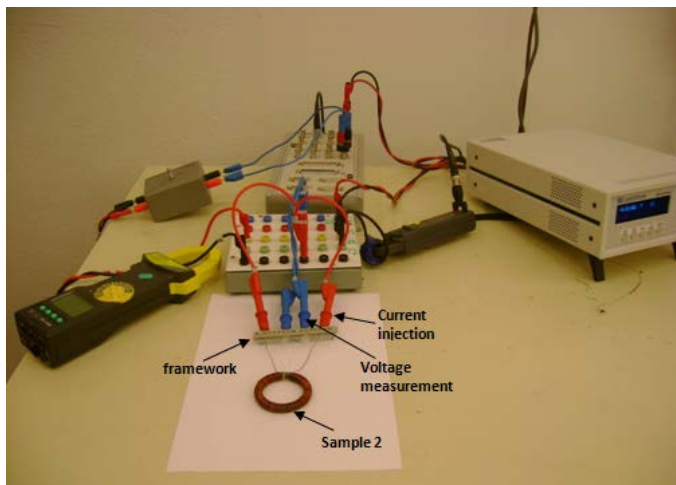


Fig. 6 Test bench arrangement for magnetic characterization of ring sample.

## 3.3 Test procedure

Prior to injection of current into the test fixture, the measuring devices were calibrated. The dc offset values from the current probes and fluxmeter were nullified.

For flux density measurement, the fluxmeter was calibrated as:

*No. of turns in excitation winding = 136*
*No. of turns in measurement winding = 533*
*Area of cross section of windings = 0.25 cm2*
*Mean magnetic path length, lm=50π mm*

The mean path length was calculated considering the middle radial path of the ring. The circumferal length was calculated using $l_m = 2 * pi * r_{middle}$ . Usually for toroid shaped samples, logarithmic functions are used. But assuming that our sample is a circular ring shaped structure with quadrature cross section, the calculation approach had been restricted to simpler means. Sinusoidal current was injected into the sample. The value of 'H' was gradually increased from 50-900 A/m. The magnetic behavior of the material was observed. At frequencies 0.1-250 Hz, the flux density levels were retrieved from the fluxmeter. The obtained signal data from B and H were analysed to calculate the area enclosed under one complete hysteresis loop. The mass of the sample was measured to be 31 g (±1 g) using an electronic pan balance. Using the area of cross section and mean magnetic path length, volume of the sample was calculated. The density of the sample was calculated to be 7894 kg/m3. Finally, the loss per cycle has been calculated according to eq. 3. The resulting total magnetic loss density [in W/Kg] the sample undergoes is calculated as product of frequency and the enclosed area of the b-h loop divided by the material density.
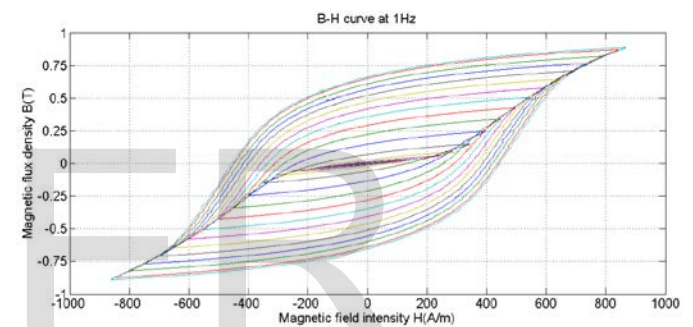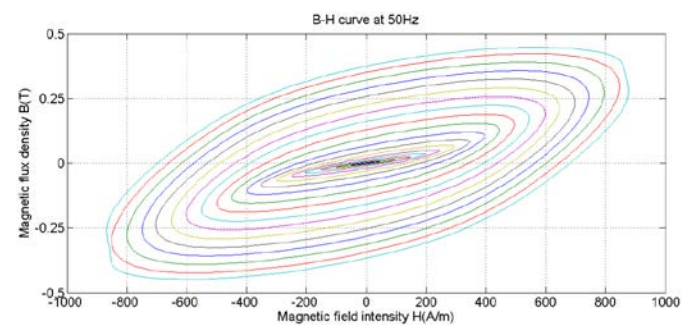
## 3.4 Obtained result and analysis

For frequency over a wide range of 0.1 – 250 Hz in conjunction with excitation level ranging from 50-900 A/m, the ring samples had been characterized. The figure sets in figure (7 a-g) shows the characteristics B-H curves for field intensity from 50 to 900 A/m.
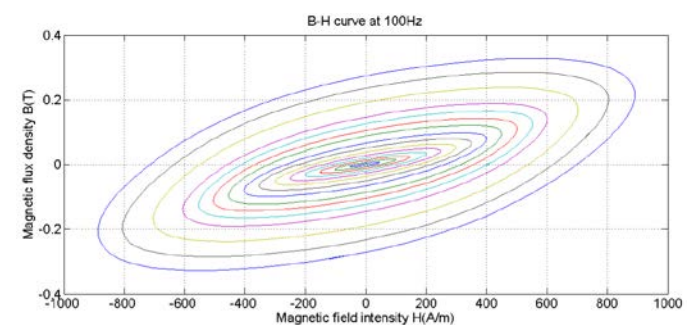


(a)



(b)



(c)
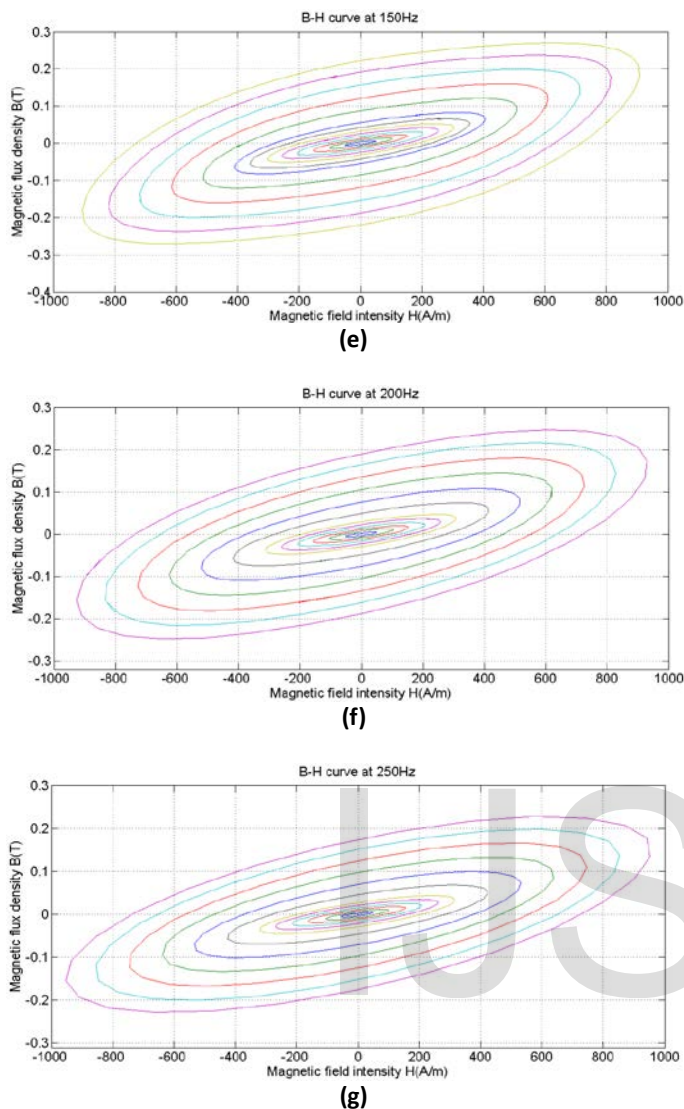


(d)

**(e)**


**(f)**


**(g)**
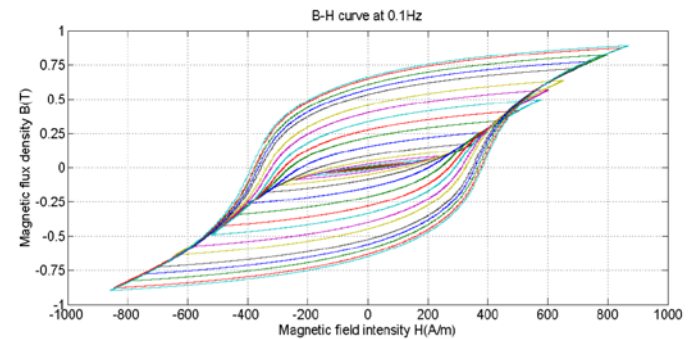
Fig. 7 a-g Characteristics B-H curves at varying frequencies

The shape of the characteristic b-h curve at low frequencies (0.1 and 1 Hz) represents mainly the hysteresis loss in the sample as shown in figure 7 a & b. Less eddy current flows, hence the sample reached higher flux density levels. With increasing field excitation, the area of the enclosed loop keeps increasing as expected from iron loss model equation in section 2.4.

The hysteresis loop at 50 Hz frequency has an elliptical in shape. Increase in loss can now be accounted not only for hysteresis loss but also for eddy currents resulting in loss. The field due to flow of eddy current opposes the applied field. The sample hence reaches lower flux density levels.

At increasingly higher frequencies (50-250 Hz), eddy current losses in the sample outweigh the losses due to hysteresis effect. The relative permeability obtained at low frequency (0.1 Hz) was approximately equal to 790. Exact value can be calculated with an initial B-H curve, provided the sample undergoes demagnetization prior to characterization.

For all the figures shown in 7a-g, the corresponding tabulated values of B, H and core loss can be found in [1].

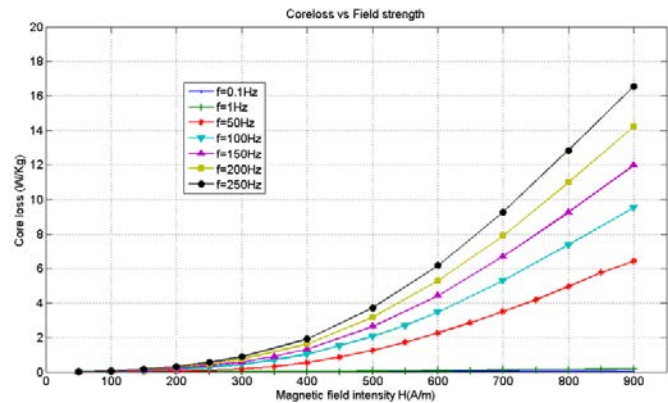The resultant plot of loss figures at different frequencies under varied excitation is shown in figure 8.


Fig. 8 Core loss under varied field excitation at different frequencies

The results shown in figure 8 clearly confirm the trend of increasing core loss at increasing frequencies under varied excitation.

As best possible alternative the measurements were performed using sinusoidal 'H'. The obtained results were found to undergo ripples and distortions. So, the signal from the power supply amplifier was analyzed for harmonics and noise contents. The spectras can be found in [1].

To verify the origin of other frequency contents, two possible sources have been checked.

- Noise from surroundings: to check the effect, the wires carrying measurement signals were twisted to reduce disturbance from the surroundings. The wires were then covered with aluminum foils to further reduce introduction of surrounding noise. But, no change was observed in the frequency components of the FFT spectrum. Hence, it was concluded that the noise originated from the amplifier itself.

- Offline filtering: An attempt was taken to perform filtering of signals to reduce the unwanted frequency contents and this worked well.

## 4 ELECTRIC CHARACTERIZATION

Electrical characterization mainly describes properties of the material such as electrical resistivity, carrier concentration, mobility, contact resistance etc. In this section, a number of experiments have been performed to measure the electrical resistivity of the ring samples.

Electrical resistivity is an important physical property for any material to be used in electrical machines. The samples, when

subjected to variable magnetic field undergo eddy current losses. Materials with high resistivity reduce eddy current loss.

## 5 MEASURING RESISTIVITY OF RING SAMPLES

Since the ring samples are toroidal with a significant thickness (5 mm) compared to effective length [12], the four point tecnique [8] and four point probe technique [9,10] could not be applied. As stated in [11], for measuring low values of resistance (in μΩ range) using multi-meters had been found ineffective. Different techniques such as four wire system and 2 wire system are available but none of them are free from contact resistance errors. The primarily performed tests came to the same conclusion too. Hence, the resistivity is measured by injecting dc current into the sample at two points equidistant to each other. The procedure is discussed in detail in the preceding section.

### 5.1 Resistivity measurement using current injection

Using similar test setup as in [8-10], constant dc current of 1 A has been injected into the sample at points 5 and 5' sitting diametrically opposite to point 5 (see figure 9). The injected current branches equally in the two half circles.
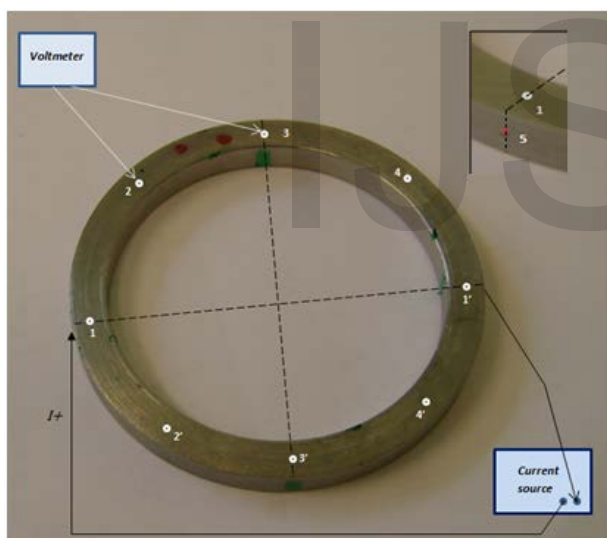


Fig. 9 Ring sample resistivity measurement setup

Voltage is measured at different points on the top surface of the sample. Measuring voltage at the points of current injection should be avoided as these results in high potential due to high current density. The electric field inside the sample is considered to be uniform according to Laplace's equation irrespective of the sample shape.

The value of electric field (V/m) and current density (A/m2) is calculated as:

$$E = -\frac{V}{d} \tag{5}$$

$$J = \frac{I/2}{A} \tag{6}$$

Where, V is the measured voltage between different points on the sample surface and d is the distance between the two voltage probes. I is the supply current and the A is the cross section area of the sample which is assumed to be constant as 5mm*5mm. Voltage is measured using Agilent 34410A multimeter [11]. Equation 6 is obtained assuming the current density to be homogeneous along the section. Current is taken as half of the supply current since it is assumed to be equally distributed in both directions along the sample.

Finally, the resistivity (Ωm) is calculated using,

$$\rho = \frac{E}{J} \tag{7}$$

### 5.2 Results

*Case 1:*

Voltage is measured at different equi-spaced points on the surface shown as white dots in figure 9. Measured voltages are shown in table 2.

TABLE 2.
MEASURED VOLTAGES BETWEEN PROBE POSITIONS

| Probe position | Measured voltage (mV) |
|---|---|
| 2-3 | 0.0872 |
| 3-4 | 0.0894 |
| 4-5 | 0.0872 |
| 5-2' | 0.0873 |
| 2-5' | 0.0861 |
| 5'-4' | 0.0881 |
| 4'-3' | 0.0854 |
| 3'-2' | 0.0866 |

For the above voltages, distance between the probes:

$$d = \frac{2\pi r_m}{8} \qquad where\ r_m = 25mm$$

The measured voltages are used in equation 5. Using equation 7, the resistivity value is calculated for the sample. The average value of resistivity in the middle semicircular path was calculated to be $\rho_m = 22.15$ μΩcm.

*Case 2:*

In case 1, resistivity of the sample was calculated in the middle path. To check the variation of resistivity along the inner and outer circular path, voltages were measured similarly to case 1. Resistivity is calculated. Results are shown in table 3.

TABLE 3
RESISTIVITY VALUE ALONG THE SURFACE BOUNDARIES

|  | Voltage (mV) | Path length (mm) | Resistivity (μΩcm) |
|---|---|---|---|
| **Inner** | 0.33 | $22.5\pi$ | 23.3 |
| **Middle** | 0.341 | $25\pi$ | 21.7 |
| **Outer** | 0.378 | $27.5\pi$ | 21.8 |

From the resulting analysis in table 3, the average resistivity of the ring samples is calculated to be approximately equal to 22.27 μΩcm over the sample surface. With increasing distance along the semicircular path 1 and 1', potential drop increases and is found maximum at semicircular arc length.

For the ring samples, the obtained value of resistivity can be further analyzed by cutting a small rectangular shaped volume of the sample and test the resistivity.

## 6 CONCLUSION

Two characterizations, magnetic and electric were performed. A brief overview of the main conclusions is presented below.

In the magnetic characterization, at increasing frequency (0.1 – 250 Hz) it undergoes higher and higher losses. The b-h curves were observed.

For the resistivity measurement of ring samples, the measured value cannot be compared since it does not have any prior characterization. But, within experimental errors and constraints, such low level resistivity measurements without using commercial devices can be considered acceptable with the conditions. Besides, the proposed resistivity measurement technique for ring shaped samples can also be adapted for other continuous shaped metallic structures.

## REFERENCES

[1] M. S. Muhit, "Magnetic and Electric Characterization of Materials for Electrical Machines", M.Sc Thesis, Royal Institute of Technology, Stockholm 2011.

[2] Fausto Fiorillo, "*Characterization and measurement of magnetic materials*", Academic Press (January 5, 2005).

[3] J. Buck, "*Automatic hysteresisgraph speeds accurate analysis of soft magnetic materials*", Proceedings of PCIM conference, February 2000.

[4] International standard, "IEC 60404-2:1996, Magnetic materials - Part 2: Methods of measurement of the magnetic properties of electrical steel sheet and strip by means of an Epstein frame".

[5] S. Zurek, P. Mareketos, T. Meydan, A.J. Moses, "*Use of novel adaptive digital feedback for magnetic measurements under controlled magnetizing conditions*", IEEE Trans. Magnetics, Vol. 41, No. 11, November 2005.

[6] A. Krings, J. Soulard, "*Overview and comparison of iron loss models for electrical machines*", Journal of Electrical Engineering, vol. 1, no. 3, pp. 162–169,  September 2010.

[7] D. Ribbenfjard, "*Electromagnetic transformer modeling including the ferromagnetic core*", Phd. Thesis, Royal Institute of Technology, Stockholm, 2010.

[8] Michael B. Heaney. "*Electrical conductivity and resistivity.*" Copyright 2000 CRC Press LLC. <http://www.engnetbase.com>

[9] F.M. Smits, "*Measurements of sheet resistivities with the four-point probe*", Bell. Syst. Tech. J. 37, 711-718 (1958)

[10] Roger Brennan & David Dickey, "*Determination of diffusion characteristics using two- and four-point probe measurements*", Solecon Lab Technical Note. <http://www.solecon.com/sra.htm>

[11] User manual, Agilent 34410A/11A 6 ½ Digit Multimeter .

[12] http://info.ee.surrey.ac.uk/Workshop/advice/coils/terms.html